Ground-state magnetization density of ^{89}Y

J. E. Wise,[1,2,*] J. R. Calarco,[1] J. P. Connelly,[1,†] S. A. Fayans,[4] F. W. Hersman,[1] J. H. Heisenberg,[1] R. S. Hicks,[3] W. Kim,[1,‡] T. E. Milliman,[1] R. A. Miskimen,[3] G. A. Peterson,[3] A. P. Platonov,[4] E. E. Saperstein,[4] and R. P. Singhal[3,§]

[1]*Department of Physics, University of New Hampshire, Durham, New Hampshire 03824*

[2]*Nuclear Physics Laboratory, Campus Box 446, University of Colorado, Boulder, Colorado 80309*

[3]*Department of Physics and Astronomy, University of Massachusetts, Amherst, Massachussetts 01003*

[4]*I. V. Kurchatov Institute of Atomic Energy, Moscow 123182, Russia*

(Received 21 September 1992)

Elastic electron scattering cross sections have been measured for ^{89}Y at 180° for $0.72 < q < 2.67$ fm^{-1}. The $M1$ form factor has been extracted and a Fourier-Bessel analysis performed to obtain the ground-state magnetization density. Calculations including effects of core polarization have been performed within the framework of the finite Fermi system theory. These show a weakening of the strong repulsion in the spin-isospin channel and are in overall agreement with the data.

PACS number(s): 25.30.Bf, 21.10.Ky, 21.60.Cs, 27.50.+e

I. INTRODUCTION

Elastic electron scattering using incident beam energies of a few hundred MeV has allowed the ground-state charge distribution to be thoroughly mapped out for a number of nuclei. These experiments have provided a stringent test for the many-body description of the nuclear ground state [1–4]. The current distributions, however, have been less systematically studied in heavy nuclei because the small cross sections for magnetic scattering are usually dominated by the large cross sections for charge scattering, even at backward angles. For nuclei with large ground-state spins, several multipoles can contribute to the scattering cross section and the individual multipole contributions cannot be easily separated. However, for nuclei with spin $\frac{1}{2}$ the scattering from the single $M1$ component may be measured and details of the nuclear structure inferred [5].

Such an example is ^{89}Y. As the ground-state spin is $j_0=\frac{1}{2}$, elastic electron scattering from ^{89}Y will contain only $C0$ and $M1$ contributions. In the extreme single-particle model, the ground state of ^{89}Y is described as a single $2p_{1/2}$ proton outside of a closed ^{88}Sr core. This is the simplest case for magnetic elastic scattering. In this model, the $C0$ form factor arises mainly from the entire static charge distribution, while the $M1$ form factor is determined mainly by the properties of the valence nucleon. A more complete model of the nuclear structure would include the effects of core polarization and short-range correlations. As the ground-state spin is experimentally observed to be $j_0=\frac{1}{2}$, the possible particle-hole combinations contributing to the core polarization are limited; such corrections to the simple model might then be thought to be a small contribution to the measured form factor.

In addition, the $M1$ form factor gives information about the contribution of meson exchange currents (MEC's). The measured magnetic moment [6] $\mu=-0.137\mu_n$ for ^{89}Y is only about half the Schmidt value $\mu=-0.26\mu_n$. As such discrepancies between one-body calculations and the experimental values of the magnetic moment have been generally attributed to MEC's [7,8], there is reason to believe that these contributions to the transverse scattering may be observable in the present case. This should be especially true at high momentum transfer, as the momentum transferred from the virtual photon to the exchanged meson is shared between two separate nucleons. Previous experiments [9,10] have shown the sensitivity of magnetic form factors to meson exchange currents as well as to core polarization contributions.

This work describes the measurement of the transverse elastic $M1$ form factor of ^{89}Y. The data were taken using the 180° scattering system [11] with the high-resolution spectrometer [12] at the Bates Linear Accelerator Center, in conjunction with a separate experiment on inelastic excitations [13]. Data were taken over a momentum transfer range of $0.72 < q < 2.67$ fm^{-1} by varying the incident energy from 71 to 262 MeV at the fixed backward scattering angle of 180°. These data were corrected for the charge scattering contribution in an off-line analysis to determine the final $M1$ form factor from the ground state. The final cross sections were further analyzed in a Fourier-Bessel analysis code to extract the corresponding magnetization current density $J_{\lambda,\lambda}$. Results are com-

*Present address: Nuclear Physics Laboratory, Campus Box 446, University of Colorado, Boulder, CO 80309.

†Present address: Department of Physics, George Washington University, Washington, D.C. 20052.

‡Present address: Nuclear Physics Laboratory, University of Illinois at Urbana-Champaign, Champaign, Illinois 61820 and Laboratory for Nuclear Science, Massachussets Institute of Technology, Cambridge, MA 02139.

§Present address: Department of Physics and Astronomy, University of Glasgow, Glasgow, G12 8QQ, Scotland.

pared with calculations within the self-consistent finite Fermi system (FFS) theory.

II. EXPERIMENT AND DATA REDUCTION

Scattered electrons were momentum analyzed with the Bates high-resolution magnetic spectrometer system [12]. Typical resolutions were 75–100 keV for the 180° data taken in this experiment. The spectrometer focal plane was instrumented with a vertical drift chamber for measurement of the momentum coordinate and vertical angle of the electron track, and a transverse array consisting of two multiwire proportional counters for measurement in the transverse direction [14]. System triggers were defined by a two out of three coincidence between two Lucite Cherenkov counters and the transverse array. Histograms of scattered electrons consistent with good scattering events were corrected for dead time and background, and then line-shape fitted to obtain the final cross sections. For momentum transfers $q \leq 1.4$ fm^{-1}, a 57.7-mg/cm^2 ^{89}Y target was used in the data collection, while a 121.9-mg/cm^2 target was used for large momentum transfers. Both had isotopic purities greater than 99% ^{89}Y. A detailed description of the experimental equipment and the method for acquiring data are given in Ref. [13] and the references therein.

The elastic differential scattering cross section for electrons from a spin-$\frac{1}{2}$ nucleus is given in plane-wave Born approximation (PWBA) by

$$\frac{d\sigma}{d\Omega}=4\pi\eta\left[\frac{d\sigma}{d\Omega}\right]_{\text{Mott}}\left[|F^C(q)|^2+\left[\frac{1}{2}+\tan^2\frac{\theta}{2}\right]|F^M(q)|^2\right], \quad (1)$$

where the form factor F^C is the Fourier-Bessel transform of the nuclear ground-state charge density $\rho(r)$,

$$F^C(q)=\int_0^\infty \rho(r)j_0(qr)r^2dr , \quad (2)$$

and F_1^M is the Fourier-Bessel transform of the $M1$ current density. For $\lambda=1$ we have

$$F_1^M(q)=\int_0^\infty J_{1,1}(r)j_1(qr)r^2dr . \quad (3)$$

Here q is the momentum transferred to the nucleus which for elastic scattering is given by

$$q=\frac{2E_i}{\hbar c}\sin\frac{\theta}{2} \quad (4)$$

for electrons of incident energy E_i scattering through a laboratory angle θ.

The nuclear recoil factor η and the Mott point cross section have been factored out in this approximation and are given by

$$\eta=\left[1+\frac{2E_i\sin^2(\theta/2)}{M_tc^2}\right]^{-1} \quad (5)$$

and

$$\left[\frac{d\sigma}{d\Omega}\right]_{\text{Mott}}=\frac{\alpha^2(\hbar c)^2\cos^2(\theta/2)}{4E_i^2\sin^4(\theta/2)} , \quad (6)$$

where M_t is the mass of the target nucleus.

At 180° the contribution from the $M1$ form factor is maximized. Charge scattering is still present, however, in all 180° systems, due to the finite acceptance of the spectrometer and straggling losses in the target. We measured the charge scattering from neighboring spin-zero nuclei at each momentum transfer point and compared the measured cross sections with the cross section predicted in the distorted-wave Born approximation from the data of Rothhaas [15]. This comparison gave a best-fit value to the effective scattering angle of 178.4°±0.1° for the 119.7-MeV data, consistent with the value of 178.5° found from a measurement of the minimum of the charge scattering parabola of ^{12}C data using the prescriptions of Rand [16] and Lapikas, Dieperink, and Box [17]. Effective target angles, spectrometer acceptances, and target thicknesses used for each momentum transfer point are given in Table I of Ref. [13].

The charge scattering contribution from ^{89}Y was determined by the measurement of the charge scattering from neighboring spin-zero nuclei. Data were acquired on a target composed of a sandwich of zirconium and molybdenum; the Zr-Mo target sandwich was composed of a 20.2-mg/cm^2 ^{90}Zr foil on top of a 19.44-mg/cm^2 ^{92}Mo metal foil, giving a target thickness approximately that of the thin yttrium target. Cross-section measurements were made under identical conditions at each momentum transfer point on this target. Corrections were made for target composition and the charge scattering differences between ^{89}Y and the spin-zero targets. This charge scattering contribution was then subtracted from the measured ^{89}Y data to obtain the transverse contribution to the scattering. Errors from the subtraction procedure were folded into the final cross sections to obtain the transverse form factors shown in Fig. 1.

Extraction of the ground-state magnetization current $J_{1,1}$ has been performed with use of a Fourier-Bessel analysis [18]. This analysis accounts for Coulomb distortion of the scattered electron in a distorted-wave Born approximation (DWBA) [19]. In Fig. 1 we have plotted the form factor as a function of effective momentum transfer

$$q_{\text{eff}}=q\left[1+\frac{4Z\alpha\hbar c}{3E_ir_0A^{1/3}}\right] , \quad (7)$$

where the radial parameter $r_0=1.12$ fm has been used for the nuclear size. This largely accounts for the effect of the Coulomb distortion on the electron plane waves.

Shown in Fig. 2 is the extracted ground-state magnetization current density $J_{1,1}(r)$. Errors shown in the figure are statistical and incompleteness errors, as well as systematic errors from the Coulomb subtraction procedure.

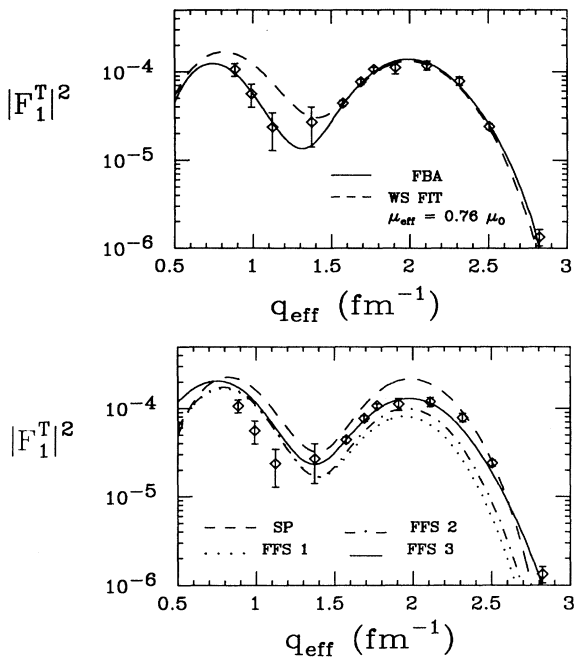

FIG. 1. (top) Transverse $M1$ form factor $|F_T|^2$ for the ground state to ^{89}Y. Contributions from $C0$ scattering have been subtracted from the experimental data as described in the text. The best fit in a Fourier-Bessel analysis is given as the solid line; the single-component Woods-Saxon fit is given by the dotted line. (bottom) Transverse $M1$ form factor with calculations from FFS theory. The dashed curve (SP) is the single-particle contribution, while the dotted curve (FFS1) includes core polarization as calculated in FFS theory. The dot-dashed curve (FFS2) is the FFS calculation with ρ-meson exchange but without a modified g', while the solid curve (FFS3) is the calculation with a q-dependent g'.

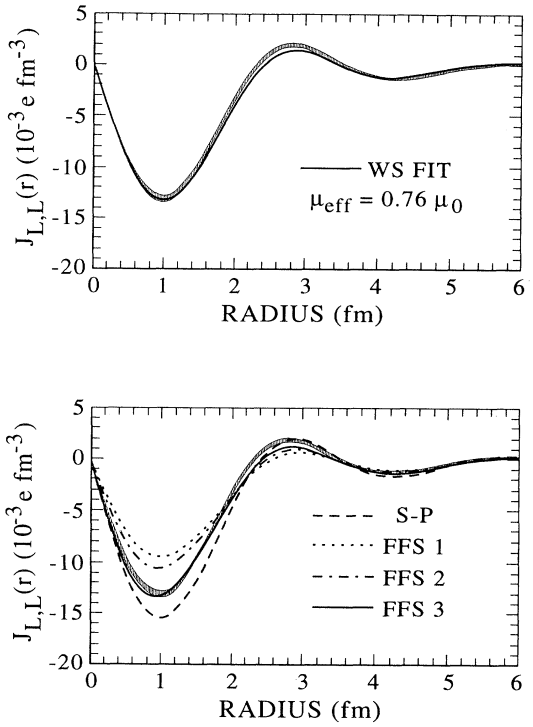

FIG. 2. (top) Current density J_{11} for the $M1$ contribution to the ground state. The solid curve is a single-particle Woods-Saxon fit. (bottom) Experimentally extracted current density for $M1$ contribution and predictions of FFS theory. The dotted curve (FFS1) is a FFS including core polarization; the dot-dashed curve (FFS2) is a FFS with explicit ρ-meson exchange but without a modified g'; the solid curve (FFS3) is the same calculation with a q-dependent g'; the dashed curve (SP) is the single-particle prediction.

III. CALCULATIONS AND INTERPRETATION

A. Phenomenological parametrization

In an independent particle-shell model, the ground state of ^{89}Y is expected to have an unpaired proton in its valence $2p_{1/2}$ orbit. We have thus performed calculations for the $M1$ contribution to the elastic scattering cross section in ^{89}Y with the assumption that the ground state consists of a single $2p_{1/2}$ proton in a Woods-Saxon central potential with a best-fit well radius of $(1.25\pm0.01)A^{1/3}$ fm. The wave function of the $2p_{1/2}$ proton and the $M1$ contribution to the elastic scattering cross section in a DWBA were calculated using the code FOUBES1 [20]. This model describes the shape of the experimental $M1$ form factor fairly well, but considerably overpredicts its strength. To fit the data, we allowed the magnetic moment of the valence proton to vary as a free parameter in the calculation of the magnetization current contribution to the DWBA cross section. This method has been shown to model the effects of core polarization and MEC's in the calculation of the $M1$ form factor of ^{207}Pb [10,21]. A value of $(0.76\pm0.04)\mu_0$ was obtained in this fit for the magnetic moment of the $2p_{1/2}$ proton in ^{89}Y, where $\mu_0=2.79\mu_n$ is the magnetic moment of a free proton.

The transverse form factor for the best fit to the magnetic moment in this single-particle model is shown as the dashed line in Fig. 1, while the best fit in the Fourier-Bessel analysis is shown as the solid line. The current extracted from the Fourier-Bessel analysis is displayed in Fig. 2 as the shaded error band.

The fit to the data in the single-particle model is reasonable above 1.5 fm^{-1}, but overpredicts the form factor by about a factor of 2 at low momentum transfers. The large χ^2 of 6.2 per degree of freedom indicates that important contributions to the cross section have been left out in this description. The Fourier-Bessel fit, on the other hand, gives a good description of the data, and thus the extracted density from this analysis represents the real density.

B. FFS theory

Microscopic calculations have been performed within the framework of the self-consistent finite Fermi system (FFS) theory [22] for both the charge and magnetization

density of the ground state of ^{89}Y. This method is, in practice, equivalent to the density functional approach with phenomenological effective forces. Calculations presented here are carried out with a modified version of the effective density functional of Ref. [23]. This modification introduces a density dependence into the finite-range forces of this functional. Its details will be given in a separate paper [24]. Here we note only that its parameters are fixed by fitting properties of several nuclei (^{40}Ca, ^{208}Pb, tin isotopes) and are not adjusted for the nucleus under consideration. The ground-state charge density generated within this approach is shown in Fig. 3, along with the experimentally extracted [25] density. The agreement with experiment is very good, except at the surface, where the calculation is somewhat enhanced as compared to the experimentally extracted density.

For the calculation of the currents within FFS theory, one should substitute the effective fields $V[J^{\mathrm{SP}}_{\lambda,\lambda'},(r)]$ for the current operators in Eq. (3), where $J^{\mathrm{SP}}(r)$ stands for the single-particle model expression for the current operator J. The effective field $V[V^0]$ arises in a nucleus when an external field V^0 is applied. It can be found by solution of the random-phase-approximation-type FFS equation, which can be written in symbolic form as

$$V[V^0]=e_q V^0+\mathcal{F}AV\ , \tag{8}$$

where e_q is a quasiparticle local charge operator with respect to the field V^0, $\mathcal{F}$ is the effective particle-hole interaction, and A stands for the particle-hole propagator, i.e., for the energy-integrated product of two quasiparticle Green's functions. The first term of Eq. (8) (with $e_q=1$) corresponds to the extreme single-particle model, whereas the second term describes the core polarization effects. It should be noted that short-range correlations are implicitly taken into account in Eq. (8) by introducing the effective interaction $\mathcal{F}$ and the local charge operator e_q. In particular, contributions from Δ-resonance–nucleon-hole virtual excitations can be treated explicitly [26] and reduced to a modification of e_q and $\mathcal{F}$. In fact, we deal here with a projection of the total Hamiltonian onto the space of particle-hole configurations. The effective interaction $\mathcal{F}$ acting in this space produces mainly long-range correlations which are taken into account by solving the FFS theory equation (8).

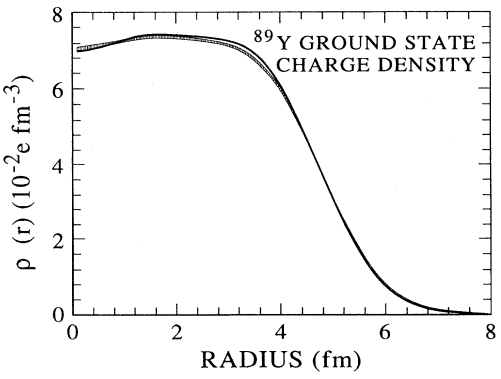

FIG. 3. Ground-state charge density for ^{89}Y as determined in Fourier-Bessel analysis. The FFS calculation is given as a solid line.

Magnetic electron scattering produces two types of external fields. The first one corresponds to the orbital current which is renormalized only by velocity-dependent forces. As it is well known that the orbital part of the magnetic moment in nuclei is very close to the bare one, we expect the renormalization of the orbital current to be small. Here we shall neglect the renormalization of the orbital current.

The second field contains the spin operator $\boldsymbol{\sigma}$: $V_n^0\propto\gamma_n\boldsymbol{\sigma}$ for neutrons and $V_p^0\propto\gamma_p\boldsymbol{\sigma}$ for protons ($\gamma_n=-1.913$ and $\gamma_p=2.793$ are the neutron and proton magnetic moments in nuclear magnetons, respectively). This field is strongly renormalized since the spin-dependent components of $\mathcal{F}$ are large. The simplest FFS ansatz for them in momentum space has the form

$$\mathcal{F}=C_0(g+g'\boldsymbol{\tau}_1\cdot\boldsymbol{\tau}_2)\boldsymbol{\sigma}_1\cdot\boldsymbol{\sigma}_2+\mathcal{F}_\pi(q)\ . \tag{9}$$

Here $C_0=\pi^2/mp_F$ is the normalization factor ($=300$ MeV fm^3 for a nucleon of mass m and average Fermi momentum p_F), $\boldsymbol{\tau}_{1,2}$ are the isospin Pauli matrices, and $\mathcal{F}_\pi$ stands for the tensor force induced by one-pion exchange in the particle-hole channel [26]:

$$\mathcal{F}_\pi=-\frac{4\pi\tilde{f}_\pi^2}{m_\pi^2}\frac{(\boldsymbol{\sigma}_1\cdot\mathbf{q})(\boldsymbol{\sigma}_2\cdot\mathbf{q})}{q^2+m_\pi^2+P_\Delta}(\boldsymbol{\tau}_1\cdot\boldsymbol{\tau}_2)\ , \tag{10}$$

where m_π is the pion mass, P_Δ stands for the Δ-isobar term of the pion mass operator, and $\tilde{f}_\pi$ is the pion-nucleon coupling constant modified by nuclear medium effects. According to the FFS prescription, $\tilde{f}_\pi$ differs from the bare coupling constant f_π by the factor $(1-2\zeta_s)$, where $\zeta_s\simeq0.1$ at small $q\leq p_F$. The Fermi momentum is here given as $p_F\simeq1.3$ fm^{-1}.

It is well known that this suppression of the spin-isospin operator is also of importance for the theoretical description of nuclear magnetic moments. ^{89}Y, the nucleus under consideration, is a good example of this. For $p_{1/2}$ nuclei, core polarization, i.e., the integral term of Eq. (8), does not significantly influence the values obtained for the magnetic moment μ [22]. By neglecting this effect, we obtain

$$\mu(p_{1/2})=\tfrac{1}{2}-\tfrac{1}{3}[\gamma_p-\tfrac{1}{2}-\zeta_s(\gamma_p-\gamma_n)]\ . \tag{11}$$

At $\zeta_s=0$, one gets the Schmidt value of $\mu_{\mathrm{Schm}}=-0.264$. This rather small μ value arises because of the strong cancellation between the orbital and spin contributions, so that a small renormalization of the spin term may lead to a noticeable change in the magnetic moment. For example, we have $\mu_{\mathrm{th}}=-0.185$ at $\zeta_s=0.05$ and $\mu_{\mathrm{th}}=-0.107$ at $\zeta_s=0.1$. By taking into account the integral term of Eq. (8), we get $\mu_{\mathrm{th}}=-0.12$ and $\mu_{\mathrm{th}}=-0.04$, respectively. Because of the high sensitivity to various small corrections, these results should be considered to be in reasonable agreement with the experimental value [6] of $\mu_{\mathrm{expt}}(^{89}\mathrm{Y})=-0.137$.

As the ρ meson is the only other isospin-1 meson entering into the N-N interaction, we have also introduced an explicit dependence on ρ-meson exchange into the spin-

isospin channel of the effective interaction [27] $\mathcal{F}$:

$$\mathcal{F}_\rho = -\frac{4\pi \tilde{f}_\rho^2}{m_\rho^2}\frac{(\sigma_1\times\mathbf{q})(\sigma_2\times\mathbf{q})}{q^2+m_\rho^2}(\tau_1\cdot\tau_2) , \tag{12}$$

where m_ρ is the ρ-meson mass and $\tilde{f}_\rho$ is the ρNN coupling constant modified by short-range NN correlations. These contributions can be approximated [27,28] by multiplying the bare ρ-coupling constant f_ρ^2 by a factor of 0.4:

$$\tilde{f}_\rho^2 = 0.4 f_\rho^2 . \tag{13}$$

FFS theory deals mainly with phenomena at small q ($q \le p_F$), where one may consider the parameters g and g' to be constant. The first of these parameters has a value close to zero, whereas g', the Landau-Migdal parameter, is about 1 [29–31]. However, the magnetic form factor is measured in electron scattering experiments for large $q \ge p_F$. For such large momentum transfers, the parametrization of $\mathcal{F}$ in the form Eq. (9) is not sufficiently well motivated. In the present case, it is more reasonable to consider the terms g and g' as q-dependent functions. It should be noted that only the second parameter is important in our calculations. Indeed, as g is small, the term proportional to g mainly determines the renormalization of the field

$$V_+^0 = V_p^0 + V_n^0 = (\gamma_p + \gamma_n)\sigma = 0.88\sigma ,$$

whereas for the term proportional to g', the field

$$V_-^0 = V_p^0 - V_n^0 = (\gamma_p - \gamma_n)\sigma = 4.7\sigma ,$$

which is larger than the first by a factor of 5.3. Therefore we shall concentrate on the amplitude g' and introduce the simplest q dependence in it as follows:

$$g'(q) = \frac{g'}{1+r_0^2 q^2} , \tag{14}$$

considering r_0^2 as a new FFS theory parameter. *A priori*, the absolute value of this parameter should be of the order of r_c^2, where r_c is the radius of the repulsive core in the N-N interaction ($\simeq 0.4$–0.5 fm).

In the FFS equation for the effective field [Eq. (8)], the particle-hole propagator A can be calculated exactly using coordinate representation [32,33]. This allows Eq. (8) to then be solved numerically without any additional approximations.

It should be noted that the term $\mathcal{F}_\pi$ does not greatly influence the magnetic form factor because of the transverse nature of the magnetic field. Indeed, in the infinite nuclear matter approximation, which is sufficiently accurate [34] for the solution of Eq. (8) at the large momentum transfers considered in this experiment, one-pion exchange induces only a longitudinal field that is $\propto(\sigma\cdot\mathbf{q})$. Consequently, in exact calculations the only contributions from $\mathcal{F}_\pi$ are from momentum nonconservation effects which cause a small mixing of the longitudinal and transverse fields.

In Ref. [35] it was shown that positions of minima and maxima of the form factor of magnetic elastic electron scattering are highly sensitive to the single-particle wave function of the odd nucleon. Therefore magnetic scattering is a probe of the self-consistent theory used for calculation of this nucleon wave function. Here, to calculate the proton $2p_{1/2}$ wave function for ^{89}Y as well as the propagator A we use the effective density functional discussed above [24].

Meson exchange currents (MEC's) modify the local charge operator e_q. At $q=0$ modifications to the charge operator were examined by Migdal [22], who showed that for the spin field the local charge is $e_q[\sigma]\approx 1$, whereas for the spin-isospin field, $e_q[\sigma\cdot\tau] = 1-2\zeta_s$, with $\zeta_s \le 0.05$–0.10. At large q ($\ge p_F$) the contributions of MEC's are known to be larger. In Ref. [5] several models for MEC's are considered. Their contributions to $|F_1^M|^2$ are found to be positive and in most cases are of the order of 20–50% (though in some models they could be higher, even up to $\approx 100\%$). Large uncertainties in the MEC contribution make it impossible to determine exactly the value of the parameter r_0^2 in Eq. (10) from the analysis of magnetic scattering. Here we omit all MEC contributions completely by putting $e_q = 1$ in Eq. (8). With this restriction, the calculation contains only one free parameter r_0^2. An estimate of the contribution of this q-dependent parameter can then be obtained from the data, keeping in mind that MEC's provide an extra positive contribution at $q(\ge p_F)$, which should be on the order of 20–50%.

Other FFS parameters are taken in accordance with Refs. [29–31]: $g=0$, $g'=1.1$. It should be noted that this value of the Landau-Migdal constant g' is in good correspondence with the Brown-Weise forces [36], which explicitly incorporate the Δ-isobar contribution with the universality assumption $g'_{NN}=g'_{N\Delta}=g'_{\Delta\Delta}=0.7$ (for details, see Ref. [26]).

The bottom part of Fig. 1 shows a set of curves for the form factor $|F_1^M|^2$ calculated within the self-consistent FFS approach (1) for the simplest single-particle (SP) approximation; (2) with core polarization taken into account through solution of Eq. (8) with the usual FFS effective interaction $\mathcal{F}$ of Eq. (9) without introducing any q dependence in g' (FFS1); (3) adding to $\mathcal{F}$ the term $\mathcal{F}_\rho$ in the form given by Eqs. (12) and (13), which is equivalent to introducing some q dependence in g' (FFS2); (4) the same as (3) but with additional explicit q dependence of g' in the form of Eq. (14) with $r_0 = 0.40$ fm (FFS3).

One can see that the single-particle model for the magnetic elastic form factor provides a reasonable description of the positions of the minima and maxima but overestimates the absolute values. This argues in favor of using the effective density functional for calculating the single-particle wave functions, as core polarization and MEC contributions will not strongly influence the positions of the minima and maxima. The calculation with $\mathcal{F}$ in the form of Eq. (9) with g' constant (FFS1) shows strong core polarization effects; as noted in Ref. [5], MEC's though highly model dependent, are found to make contributions on the order of 20–50% to the transverse form factor. As our data indicates a factor of about 2.6 difference between the core polarization calculation and the data at a momentum transfer of 2.5 fm^{-1}, alternative explanations for the excess strength should be explored. An alterna-

tive method to reproduce this excess strength would be to introduce a q dependence into the constant g', which is equivalent to introducing a q dependence into the strong short-range repulsion in the spin-isospin channel. Inclusion of $\mathcal{F}_\rho$ leads to some weakening of the central part of the spin-isospin repulsion at high q. Indeed, using the vector identity

$$(\boldsymbol{\sigma}_1\times\mathbf{q})\cdot(\boldsymbol{\sigma}_2\times\mathbf{q})=(\boldsymbol{\sigma}_1\cdot\boldsymbol{\sigma}_2)q^2-(\boldsymbol{\sigma}_1\cdot\mathbf{q})(\boldsymbol{\sigma}_2\cdot\mathbf{q}) ,$$

it can be easily seen that the addition of the term $\mathcal{F}_\rho$ into Eq. (9) gives an additional contribution to the tensor term [Eq. (10)] and is thus equivalent to the introduction of some q dependence to the Landau-Migdal parameter g'. As the second term is $\propto(\boldsymbol{\sigma}\cdot\mathbf{q})$, it introduces only a longitudinal field, and just as in the case of the pion exchange force $\mathcal{F}_\pi$, it does not noticeably influence the magnetic form factor. The first term, however, is negative, and therefore the total effect of the introduction of an explicit ρ dependence is to improve the fit to the data (curve FFS2). However, the effect is not strong enough to give an adequate description of the data, especially at $q\geq 2.5$ fm^{-1}. Finally, the introduction of an additional explicit q dependence in g' of Eq. (14) with $r_0=0.4$ fm (FFS3) gives a result which is consistent with the data in the region above $q\approx 1.5$ fm^{-1}, leaving some room for MEC contributions and other small corrections. These could include a mixture of additional shell-model configurations to the main, single-particle one as well as relativistic effects, which are left out of the present calculation. It should be mentioned that for low-q region, the MEC contributions should suppress the theoretical curves for the form factor by the factor of $(1-2\zeta_s)^2\approx 0.64$.

An analogous set of curves is given in the bottom part of Fig. 2 for the magnetic current density $J_{\lambda,\lambda}(r)$. An examination of these curves leads to similar conclusions for the currents, though here the influence of the momentum transfer dependence of the effective interaction is not as transparent as above. It should be noted that the diminishing of the interaction strength g' at large q is confirmed also by the analysis of elastic electron magnetic scattering from ^{207}Pb, where the valence neutron is in the $3p_{1/2}$ state and in ^{41}Ca [37]. This analysis also confirms the above estimate for the parameter r_0.

IV. CONCLUSIONS

Elastic electron scattering data have been acquired at a 180° scattering angle for momentum transfers $0.72<q<2.67$ fm^{-1}. From these data, the magnetization current density for the $M1$ component of the ground state of ^{89}Y has been extracted. The data were further analyzed within a phenomenological shell model and within a microscopic approach using the self-consistent FFS theory. The phenomenological model describes the ground state of ^{89}Y as a single $2p_{1/2}$ proton outside of a closed core. This model predicts the shape of the extracted $M1$ form factor fairly well, but overpredicts its strength. A quenching of the effective magnetic moment of the valence $2p_{1/2}$ proton, introduced to model the effect of core polarization and MEC contributions, provides the necessary reduction of the cross section above 1.5 fm^{-1}, but is found to be an inadequate model to describe the data, especially at low momentum transfer.

The FFS calculations take into account core polarization effects, but do not consider MEC contributions. If the MEC's are relatively small (20–50%), the analysis demonstrates a weakening of the strong repulsion in the spin-isospin channel (Migdal parameter g') for $q\geq 1$ fm^{-1}. A q dependence for this interaction amplitude was introduced with a new parameter r_0, which can be interpreted as the effective radius of the interaction in the spin-isospin channel. This parameter is estimated from the analysis and found to be about 0.4 fm. With this additional q-dependent term, the FFS calculations are found to be in overall agreement with the data, leaving some room for the MEC contributions and other small corrections.

ACKNOWLEDGMENTS

The authors would like to thank the staff of the MIT-Bates Linear Accelerator Center for their help and support. Special thanks also goes to R. J. Peterson for his generous support of this work. This work was supported in part by the U.S. Department of Energy under Contract Nos. DE-FG02-88ER40410, DE-FG02-88ER40415, and DE-FG02-86ER-40269.

[1] R. Hofstadter, Annu. Rev. Nucl. Part. Sci. **7**, 231 (1957).
[2] T. deForest and J. D. Walecka, Adv. Phys. **15**, 1 (1966).
[3] H. Überall, *Electron Scattering from Complex Nuclei* (Academic, New York, 1971).
[4] B. Frois and C. N. Papanicolas, Annu. Rev. Nucl. Part. Sci. **37**, 133 (1987).
[5] T. W. Donnelly and I. Sick, Rev. Mod. Phys. **56**, 461 (1984).
[6] C. Hassler, J. Kronenbitter, and A. Schwenk, Z. Phys. A **280**, 117 (1984).
[7] F. Villars, Helv. Phys. Acta **20**, 476 (1947).
[8] H. Miyazawa, Prog. Theor. Phys. **6**, 801 (1951).
[9] S. K. Platchkov, J. B. Bellicard, J. M. Cavedon, B. Frois, D. Goutte, M. Huet, P. Leconte, Phan Xuan-Ho, P. K. A. de Witt Huberts, L. Lapikas, and I. Sick, Phys. Rev. C **25**, 2318 (1982).
[10] C. N. Papanicolas, L. S. Cardman, J. H. Heisenberg, O. Schwentker, T. E. Milliman, F. W. Hersman, R. S. Hicks, G. A. Peterson, J. S. McCarthy, J. Wise, and B. Frois, Phys. Rev. Lett. **58**, 2296 (1987).
[11] G. A. Peterson, Nucl. Instrum. Methods **59**, 341 (1968); G. A. Peterson and W. C. Barber, Phys. Rev. **128**, 812 (1962); G. A. Peterson, J. B. Flanz, D. Webb, Hans de Vries, and C. F. Williamson, Nucl. Instrum. Methods **160**, 375 (1979).
[12] W. Bertozzi, M. V. Hynes, C. P. Sargent, W. Turchinetz, and C. Williamson, Nucl. Instrum. Methods **162**, 211 (1982).
[13] J. E. Wise, F. W. Hersman, J. H. Heisenberg, T. E. Milliman, J. P. Connelly, J. R. Calarco, and C. N. Papanicolas,

Phys. Rev. C **42**, 1077 (1990).
[14] W. Bertozzi, M. V. Hynes, C. P. Sargent, C. Creswell, P. C. Dunn, A. Hirsch, M. Leitch, B. Norum, F. N. Rad, and T. Sasanuma, Nucl. Instrum. Methods **141**, 457 (1977).
[15] H. Rothhaas, Ph.D. thesis, University of Mainz, 1970, unpublished and private communication.
[16] R. E. Rand, Nucl. Instrum. Methods **39**, 45 (1966).
[17] L. Lapikas, A. E. L. Dieperink, and G. Box, Nucl. Phys. **A203**, 609 (1973).
[18] J. Heisenberg, in *Advances in Nuclear Physics,* edited by J. Negele and E. Vogt (Plenum, New York, 1981), p. 61; J. Heisenberg and H. P. Blok, in *Annual Review of Nuclear and Particle Science,* edited by J. D. Jackson, H. E. Gove, and R. F. Schwitters (Annual Reviews, Palo Alto, 1983), p. 569.
[19] H. C. Lee, Atomic Energy of Canada Limited Report No. AECL-4839, 1975.
[20] J. H. Heisenberg, code FOUBES1 (unpublished).
[21] T. Suzuki, M. Oka, H. Hyuga, and A. Arima, Phys. Rev. C **26**, 750 (1982).
[22] A. B. Migdal, *Theory of Finite Fermi Systems and Properties of the Atomic Nucleus* (Wiley, New York, 1967).
[23] A. V. Smirnov, S. V. Tolokonnikov, and S. A. Fayans, Yad. Fiz. **48**, 1661 (1988) [Sov. J. Nucl. Phys. **48**, 995 (1988)].
[24] S. A. Fayans (unpublished).
[25] S. A. Fayans and V. A. Khodl, Pis'ma Zh. Eksp. Teor. Fiz. **17**, 633 (1973) [JETP Lett. **17**, 444 (1973)].
[26] A. B. Migdal, E. E. Saperstein, M. A. Troitsky, and D. N. Voskresensky, Phys. Rep. **192**, 179 (1990).
[27] J. Speth, V. Klemt, J. Wambach, and G. E. Brown, Nucl. Phys. **A343**, 382 (1980).
[28] G. E. Brown, E. Osnes, and M. Rho, Phys. Lett. **163B**, 41 (1985).
[29] I. N. Borzov, S. V. Tolokonnikov, and S. A. Fayans, Yad. Fiz. **40**, 1151 (1984) [Sov. J. Nucl. Phys. **40**, 732 (1984)].
[30] N. I. Pyatov and S. A. Fayans, Fiz. Elem. Chastits At. Yadra **14**, 953 (1983) [Sov. J. Part. Nucl. **14**, 401 (1983)]; F. A. Gareev, S. N. Ershov, N. I. Pyatov, and S. A. Fayans, *ibid.* **19**, 373 (1988) [**19**, 373 (1988)].
[31] J. Bang, S. A. Fayans, F. A. Gareev, S. N. Ershov, and N. I. Pyatov, Nucl. Phys. **A440**, 445 (1985).
[32] E. E. Saperstein, S. V. Tolokonnikov, and S. A. Fayans, I. V. Kurchatov Institute of Atomic Energy Report No. 2571, Moscow, 1975.
[33] S. Shlomo and G. Bertsch, Nucl. Phys. **A243**, 507 (1975).
[34] S. A. Fayans, E. E. Saperstein, and S. V. Tolokonnikov, Nucl. Phys. **A326**, 463 (1979).
[35] R. N. Kasymbalinov and E. E. Saperstein, Yad. Fiz. **53**, 1273 (1991) [Sov. J. Nucl. Phys. **53**, 784 (1991)].
[36] G. E. Brown and W. Weise, Phys. Rep. **27**, 1 (1976).
[37] W. Kim, A. P. Platonov, and E. E. Saperstein, Yad. Fiz. **56** (to be published).